

Research Article

High Operating Voltage Supercapacitor Using PPy/AC Composite Electrode Based on Simple Dipping Method

Kyoungho Kim

*School of Energy & Chemical Engineering, Ulsan National Institute of Science and Technology (UNIST),
UNIST-gil 50, Ulsan 689-798, Republic of Korea*

Correspondence should be addressed to Kyoungho Kim; khkimecl@gmail.com

Received 3 August 2015; Accepted 13 October 2015

Academic Editor: Frederic Dumur

Copyright © 2015 Kyoungho Kim. This is an open access article distributed under the Creative Commons Attribution License, which permits unrestricted use, distribution, and reproduction in any medium, provided the original work is properly cited.

As various wearable devices are emerging, self-generated power sources, such as piezoelectric generators, triboelectric generators, and thermoelectric generators, are of interest. To adapt self-generated power sources for application devices, a supercapacitor is necessary because of the short generation times (1–10 ms) and low generated power (1–100 μ W) of self-generated power sources. However, to date, supercapacitors are too large to be adapted for wearable devices. There have been many efforts to reduce the size of supercapacitors by using polypyrrole (PPy) for high energy supercapacitor electrodes. However, these supercapacitors have several disadvantages, such as a low operating voltage due to the use of an aqueous electrolyte, and complex manufacturing methods, such as the hydrogel and aerosol methods. In particular, the low operating voltage (\sim 1.0 V) is a significant issue because most electronic components operate above 3.0 V. In this study, we successfully demonstrated the high operating voltage (3.0 V) of a supercapacitor using a PPy/activated carbon (AC) composite electrode based on the chemical polymerization of the PPy by simple dipping. In addition, a twofold enhancement of its energy density was achieved compared with conventional supercapacitors using AC electrodes.

1. Introduction

As various wearable devices are emerging, for example, smart watches, smart bands, and activity trackers [1, 2], their energy sources are quite important. These wearable devices are operated on parts of the human body, such as the neck, wrist, and chest; therefore, it is necessary that their energy sources have a small size, low thickness, high power, and high energy for the various operating functions of the wearable devices. Unfortunately, existing batteries cannot completely satisfy these requirements. To overcome these issues, many researchers have endeavored to develop self-generated power sources such as piezoelectric generators, triboelectric generators, and thermoelectric generators [3–5]. However, self-generated power sources have drawbacks, such as a short generation time (1–10 ms), low generated power (1–100 mW), and nonregularized power. These issues could be resolved by using supercapacitors that can rapidly charge and discharge. A hybrid energy storage system that consists of a supercapacitor and battery has recently been of interest [6, 7].

To successfully demonstrate a hybrid energy storage system, the energy density of supercapacitors has to be improved because the energy density of existing supercapacitors is relatively low (10–20 F/g).

To increase the energy density of the supercapacitors, many studies involving composite electrodes fabricated from materials such as metal oxide/activated carbon (AC) [8], conducting polymer/carbon [9–11], and carbon derivatives [12, 13] have been conducted. In particular, conducting polymers have been used for various functions, such as conducting agents, highly porous materials, and redox reaction sources for polymer/AC composite electrodes. For example, Sun and Mo [14] reported a specific capacitance of 238 F/g, which is approximately ten times higher than that of commercial supercapacitors using just AC electrodes. However, the majority of these reported results were based on the use of aqueous electrolytes, such as H_2SO_4 , KOH, NaCl, and Na_2SO_4 . Given that most of the electronic components of wearable devices operate at 3.0 V (some sensors are able to partially operate at 1.5 V), aqueous supercapacitors can be

used when connected in series of three. However, wearable devices do not allow sufficient space for a supercapacitor to be used. Moreover, aqueous supercapacitors have complex manufacturing methods, such as the hydrogel [15] and aerosol methods [16].

In this study, we successfully demonstrated a nonaqueous supercapacitor based on a PPy/AC composite electrode with a high operating voltage (3.0 V). We prepared that PPy/AC composite electrode was made by a chemical polymerization, which was carried out via dipping into pyrrole monomer solution and dopant (1.0 M tetraethylammonium p-toluenesulfonate in an acetonitrile) solution, sequentially. And we assembled and tested the nonaqueous cylindrical supercapacitor, which was prepared by winding of the composite electrodes. As a result, we achieved a twofold enhancement of the energy density compared with that of conventional supercapacitors based on AC, with a capacity reduction of 17% over 2,500 cycles. Furthermore, to prepare the composite electrode for the supercapacitor, we used a chemical polymerization method via a simple dipping method. Therefore, these developmental results could be directly applied to a mass production process. Given these advantages, this supercapacitor based on a PPy/AC composite electrode should be a promising energy source for wearable devices.

2. Materials and Methods

Mixtures of active material, electric conductive material, and binding materials were prepared using fixed ratios of 75:15:10. Carbon black was used as the electric conductive material. Styrenebutadiene rubber, polytetrafluoroethylene, carboxymethylcellulose, and polyvinylpyrrolidone were used as water-soluble binding materials. AC was used as the active material. All materials were purchased from Sigma-Aldrich. In all cases, the electrode materials were mixed using distilled water as a solvent. The slurries were prepared by agitating the mixtures via a ball-mill method at a speed of 200 rpm for 6 h. The mixing was performed at room temperature. Using Dr. Blade method, the well-mixed slurries were evenly coated onto both sides of a 20 μm thick etched-aluminum foil. The prepared electrodes were dipped in pyrrole monomer and air-dried. Subsequently, the prepared electrodes were also dipped in 1.0 M tetraethylammonium p-toluenesulfonate (TEApTS) in an acetonitrile (ACN) solution and air-dried.

The supercapacitors were prepared as follows: the prepared PPy/AC composite electrodes were cut to a size of 2 \times 5 cm and compressed at a pressure of 0.7–0.8 ton cm^{-2} at 120°C. The cylindrical elements were prepared by stitching the terminals and winding them in the presence of the separation films. The manufactured cylindrical elements were dried at 120°C for 48 h under vacuum conditions of 30 mbar or less. Subsequently, they were sufficiently impregnated in 1.0 M tetraethylammonium tetrafluoroborate (Et_4NBF_4) in an ACN electrolyte within a glovebox filled with argon gas. Finally, the supercapacitors were sealed by inserting rubber caps into the glovebox.

The materials were examined with the use of a particle size analyzer (PSA), Brunauer-Emmett-Teller (BET) analysis,

and scanning electron microscopy (SEM). The particle size and pore distributions prior to and following the ball-milling process were determined using PSA and BET analysis. SEM analysis was conducted to observe the surface of the electrode. For the electrochemical measurement, cyclic voltammetry (CV) and galvanostatic charge-discharge studies of the supercapacitors employing the PPy/AC composite electrodes and the AC electrodes, respectively, were conducted using an EG&G Model 273A Potentiostat/Galvanostat, Princeton Applied Research. AC-impedance analysis was performed using an electrochemical impedance analyzer at a voltage of $\pm 1\text{ mV}$ and a frequency range of 0.01–100,000 Hz. Following the discharge of the supercapacitors at various current densities, the specific capacitance and energy density of the supercapacitors were also measured using a cycler. In addition, the reliability of the supercapacitors over 2,500 cycles was determined by a charge/discharge experiment.

3. Results and Discussions

Figure 1 shows the schematic illustration for the preparation of the PPy/AC composite electrodes and the nonaqueous cylindrical supercapacitor. The PPy/AC composite electrodes were fabricated by a simple process consisting of ball-mill mixing, Dr. Blade coating, and dipping into pyrrole monomer and TEApTS/ACN solutions used as dopants (Figure 1(a)). The prepared PPy/AC composite electrodes were wound using a homemade winding machine, and following the impregnation of 1.0 M $\text{Et}_4\text{NBF}_4/\text{ACN}$ (Figure 1(c)), the supercapacitors were sealed by inserting rubber caps in glovebox.

To examine the properties of the electrode materials, the materials were analyzed by PSA, BET, and SEM. Table 1 shows the BET data of the active materials for the electrodes. The AC electrode had large surface and mesopore areas of 1867.93 $\text{m}^2\text{ g}^{-1}$ and 202.57 $\text{m}^2\text{ g}^{-1}$, respectively. In addition, the mesopore ratio was determined as 11%. These values demonstrate that a large surface area is available to facilitate high electric double layer capacitance led by a nonfaradaic reaction. From these values, we were able to predict that a high capacity could be achieved. Figures 2(a) and 2(b) show the particle size distributions of the AC, the conductive carbon, and the mixtures prepared using the ball-mill method. The average particle sizes of the AC and conductive carbon were 30 and 5 μm , respectively. To achieve a uniform particle size, ball-mill mixing was performed at 200 rpm for 6 h; following this process, the particles of the mixture had a uniform average size of approximately 10 μm . The surface morphologies of the AC electrode and PPy/AC composite electrode are shown in Figures 2(c) and 2(d). In the SEM image of the AC electrode, relatively uniform active particles and many pores can be observed. The high capacitance can be attributed to these pores. Following dipping in the pyrrole monomer solution and TEApTS/ACN solution, small PPy particles were observed and the redox reaction may be encountered by them.

Owing to the redox reaction of the PPy, the PPy/AC composite electrode with a high surface area is expected to display improved electrochemical capacitive properties compared

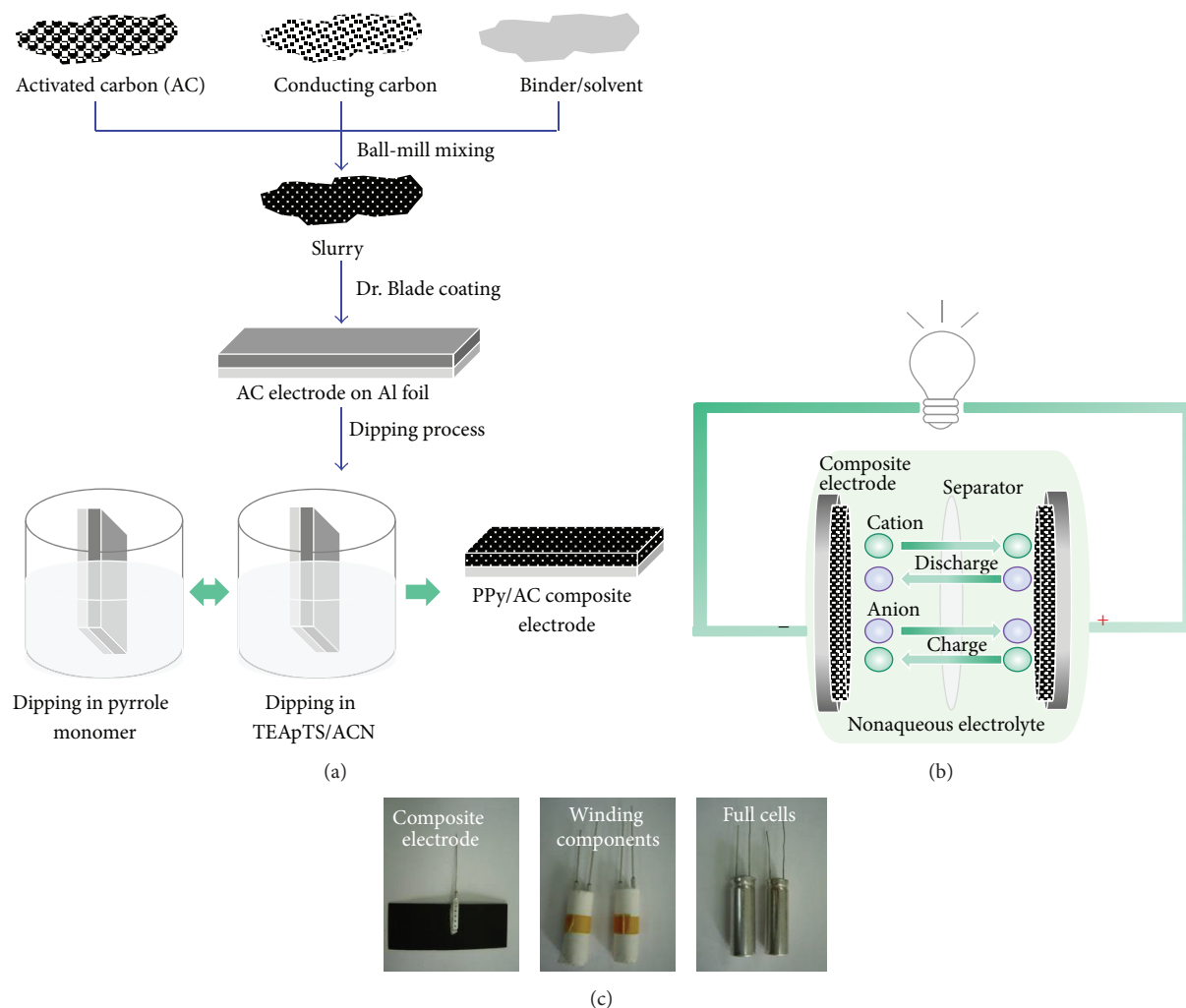


FIGURE 1: (a) Schematic illustration of the preparation of the PPy/activated carbon composite electrode. (b) Schematic illustration of the nonaqueous supercapacitor. (c) Digital photography of the components for the nonaqueous supercapacitor.

TABLE 1: BET data of the active materials for the electrodes before and after ball-mill mixing.

Contents	Unit	Before ball-mill mixing		After ball-mill mixing
		Activated carbon	Conductor carbon	
Total surface area	m^2/g	1867.93	67.62	1987.03
Mesopore area	m^2/g	202.57	61.43	193.57
Total pore volume	m^3/g	0.89	0.137	0.79
Mesopore volume	m^3/g	0.14	0.135	0.12
Mesopore ratio	%	11	91	9.7
Mesopore volume ratio	%	16	99	15.2
Average diameter	\AA	29.01	5.3	19.01

with conventional AC electrodes. The electrochemical capacitance of the supercapacitor based on the PPy/AC composite electrode was calculated by a galvanostatic charge-discharge profile. Figure 3(a) shows the charge-discharge curves at various current densities ranging from 0.5 to 5.0 A g^{-1} between voltages of 0.0–3.0 V. The rapid charge/discharge process is facilitated by the electrochemisorption of the electrolyte

cations (Et_4N^+) at the negative electrode and the electrolyte anions (BF_4^-) at the positive electrode, along with the formation of an electric double layer. Noticeably, the calculated specific capacitance (45.1 F g^{-1}) was determined to be constant at various current densities up to 0.5 A g^{-1} . This significantly high capacitance could be attributed to the high surface area and redox reaction of the PPy/AC composite electrode [22].

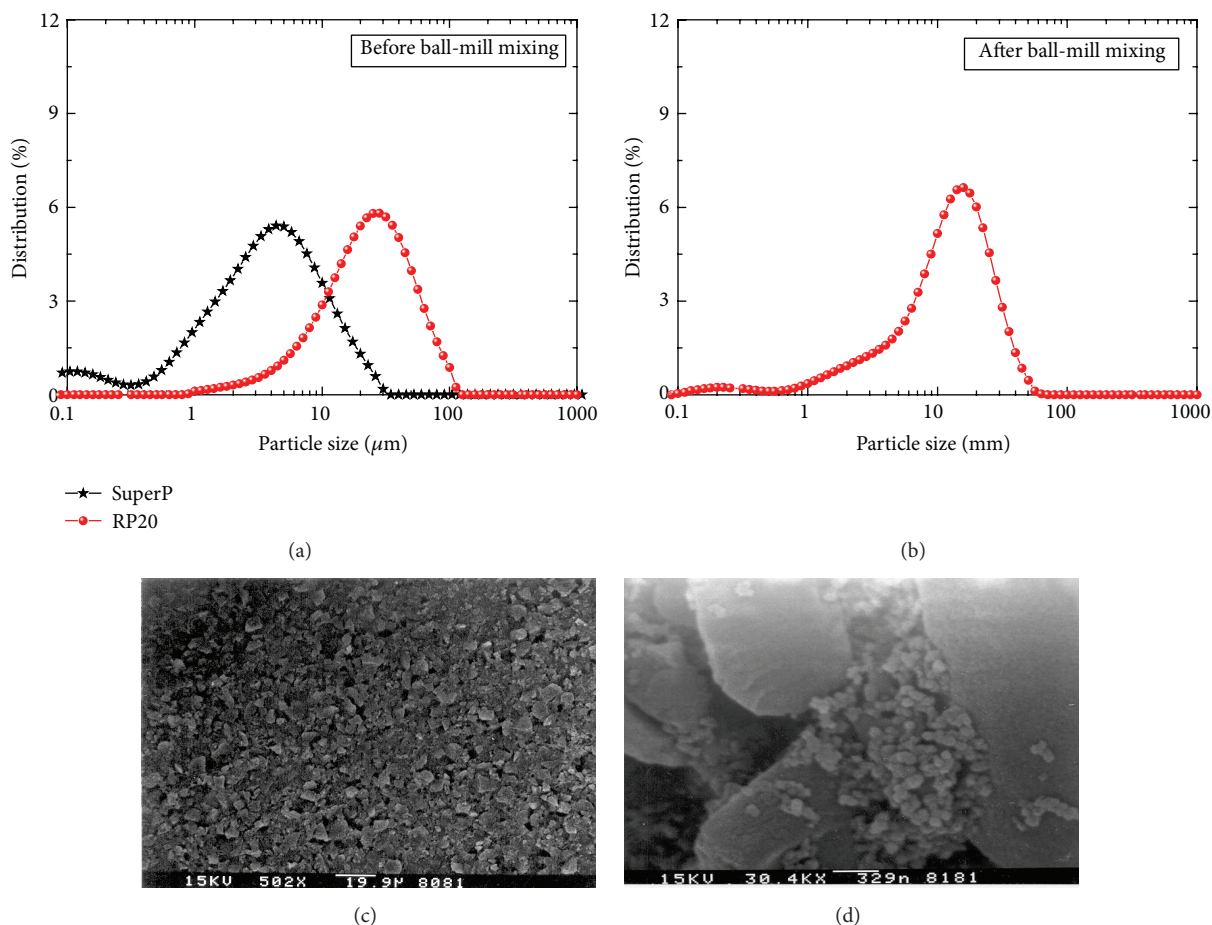


FIGURE 2: (a) and (b) PSA data of the active materials for the electrodes before and after ball-mill mixing. (c) and (d) Surface SEM images of the electrode.

Remarkably, we successfully demonstrated a high operating voltage of 3.0 V, and it can be clearly observed that our supercapacitor based on the PPy/AC composite electrode shows a superior operating voltage performance to most previously reported supercapacitors based on PPy electrodes. CV was performed to evaluate the electrochemical behavior of the supercapacitor based on the PPy/AC composite electrode in nonaqueous Et_4NBF_4 within an ACN electrolyte at various scan rates ranging from 20 to 500 mV s^{-1} . The CV plots show a quasi-rectangle shape, characteristic of a typical supercapacitor, even at a high scan rate of 500 mV s^{-1} (Figure 3(b)).

The Nyquist plots of the supercapacitors based on the PPy/AC composite electrode were obtained from the AC-impedance analysis (Figure 3(c)). A polarization effect is observed at high frequency (1,000–100,000 Hz) for most electrochemical devices that exhibit a faradaic reaction; therefore, a semicircle could be observed. At low frequency (0.01–10 Hz), a mass transfer effect is observed and a line, parallel to the imaginary axis or at an angle of less than 90° to the real axis in the Nyquist plot, is exhibited. At a moderate frequency (10–1,000 Hz), a polarization effect, mass transfer effect, or superposition effect was observed for supercapacitors. In the case of the superposition effect, the behavior of the Warburg

impedance or the incomplete semicircle is revealed [8]. The supercapacitor based on the PPy/AC composite electrode demonstrated semicircle shapes owing to the polarization at high frequency and vertical lines owing to the mass transfer at low frequency. These behaviors are known to be due to the redox reaction of the PPy. The ohmic resistance values of the supercapacitor were approximately $0.2 \text{ m}\Omega$. To evaluate its cyclic stability, we have also investigated the cyclic charge-discharge properties over 2,500 cycles at 5 A g^{-1} for the PPy/AC composite electrode, as shown in Figure 3(d). Notably, it was observed that the supercapacitor based on the PPy/AC composite electrode retains approximately 87% of its initial specific capacitance over 2,500 cycles.

To confirm the superiority of the supercapacitor based on the PPy/AC composite electrode, we performed electrochemical tests to compare its performance with that of the conventional supercapacitor based on the AC electrode. Figure 4(a) shows the galvanostatic charge-discharge curves of the supercapacitors based on the PPy/AC composite electrode and AC electrode. The supercapacitor based on the PPy/AC composite electrode is able to charge to voltages ranging from 0.0 to 3.0 V; however, the supercapacitor based on the AC electrode cannot charge to the same voltage range because of undesired side reactions. However, the curves

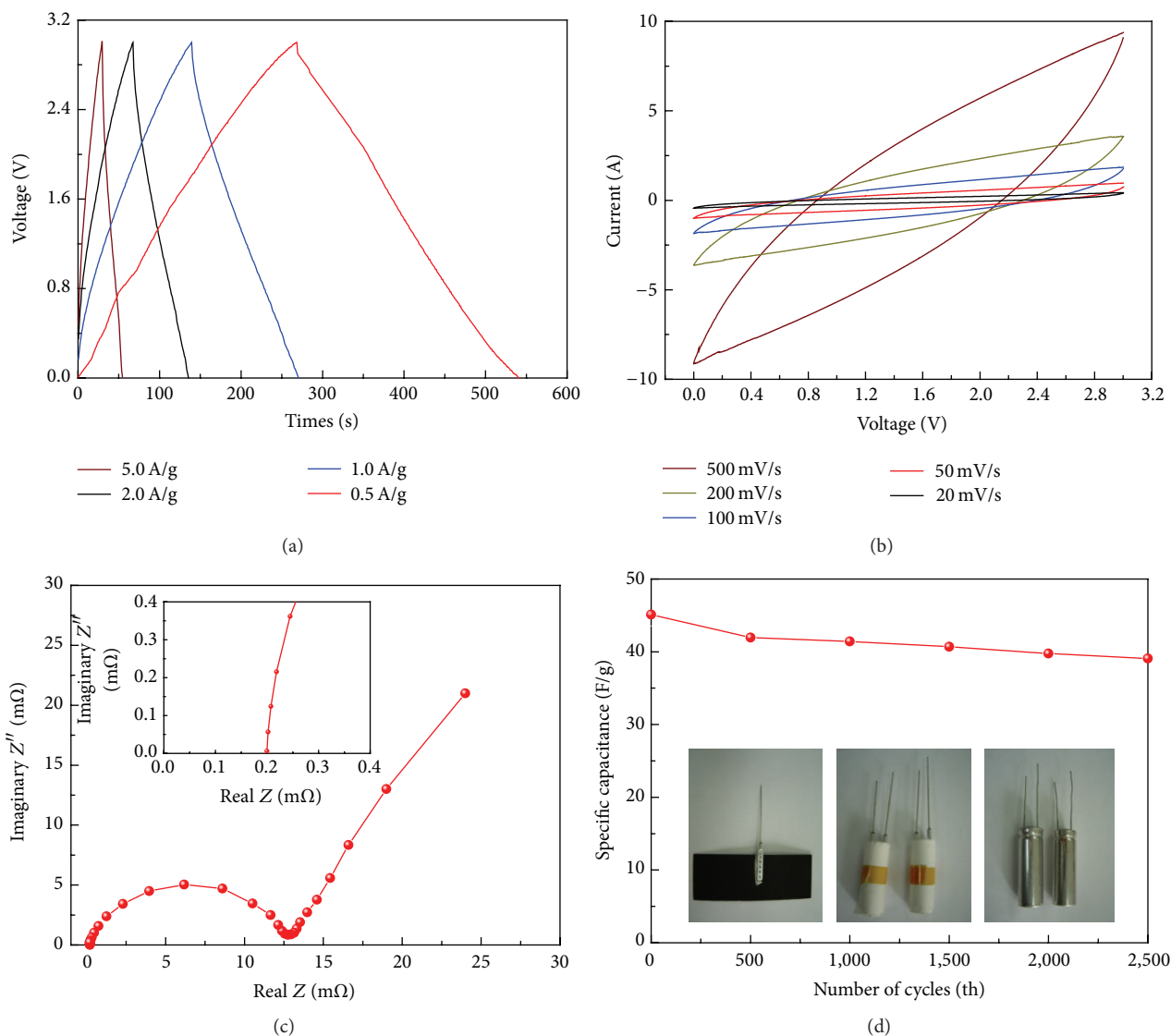


FIGURE 3: Electrochemical analysis of the supercapacitor based on PPy/AC composite electrode in nonaqueous electrolyte. (a) Galvanostatic charge-discharge profile at different current density. (b) CV curves at different scan rates. (c) Nyquist plot. (d) Cyclic stability test up to 2500 cycles at 5 A g⁻¹ current density.

of both supercapacitors exhibited a symmetric reverse V-shape. The Nyquist plots of the supercapacitors based on the PPy/AC composite electrode and the AC electrode are shown in Figure 4(b). As previously mentioned, the plot for the supercapacitor based on the PPy/AC composite electrode exhibited a semicircle due to the redox reaction of the PPy. However, the plot for the supercapacitor based on the AC electrode did not exhibit any semicircles due to the polarization at a high frequency, but vertical lines were observed due to the mass transfer at low frequency; this is typical for a conventional supercapacitor. Considering the cyclic stability of the supercapacitors, the capacitance retention of the supercapacitors using the PPy/AC composite and the AC electrodes was 87% and 92%, respectively (Figure 4(c)).

Figure 4(d) presents a Ragone plot, which demonstrates the relationship between the energy density and power density of the supercapacitor. The supercapacitor based on the PPy/AC composite electrode delivered a maximum energy density of 56.4 Wh kg⁻¹ at a power density of 30 W kg⁻¹, and it maintained a value of 18.8 Wh kg⁻¹ at a high power density of 20,000 W kg⁻¹. However, for the broader context of our work, the operating voltage and energy density of our supercapacitor based on the PPy/AC composite electrode were compared with other reported supercapacitors based on PPy; the results are shown in Table 2. From Table 2, it can be clearly observed that the supercapacitor based on the PPy/AC composite electrode demonstrated a better performance than most previously reported supercapacitors [17–21].

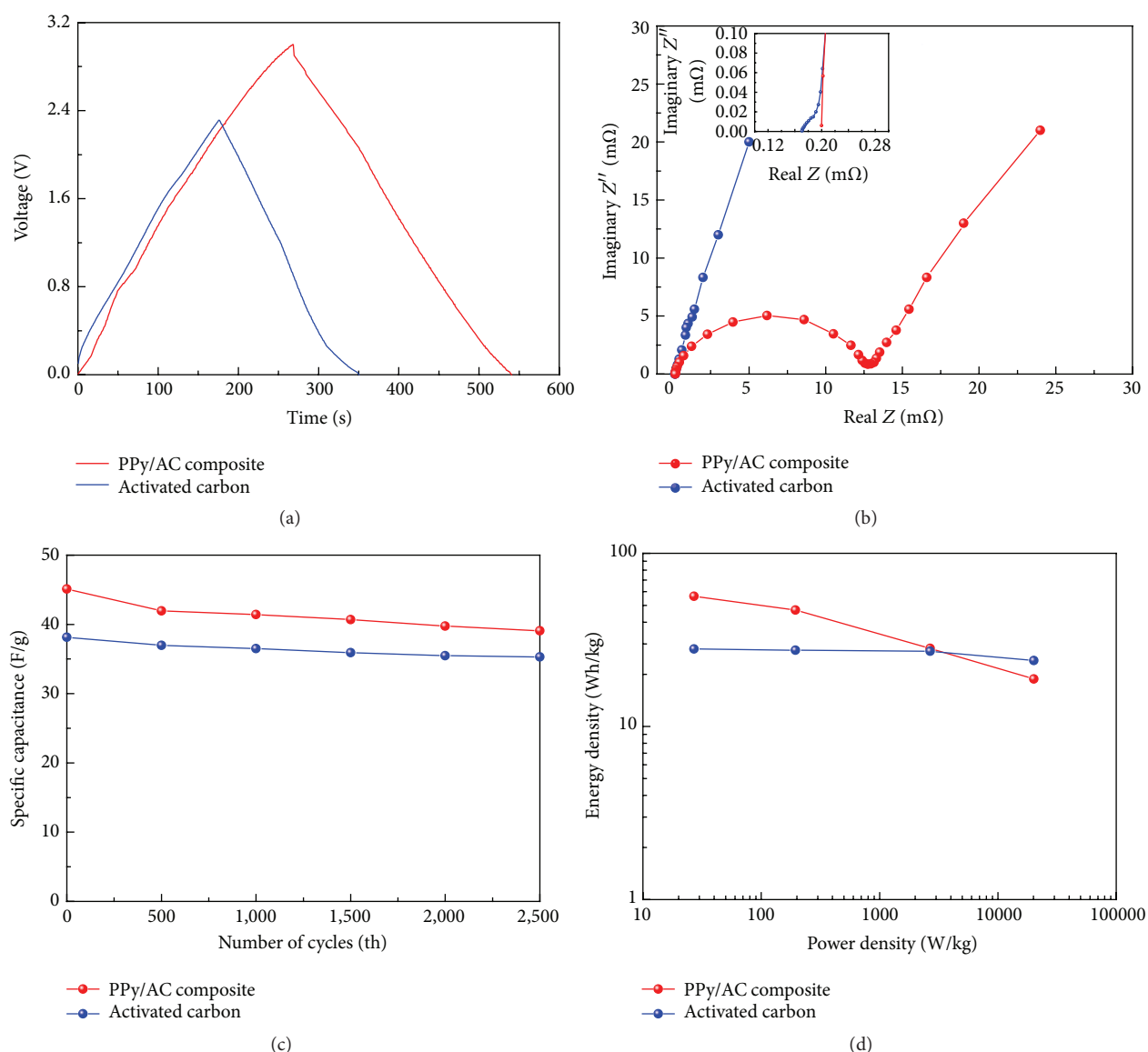


FIGURE 4: Comparison with electrochemical properties of supercapacitors using PPy/AC composite electrode and activated carbon electrode. (a) Galvanostatic charge-discharge curves. (b) The Nyquist plots. (c) Cyclic stability test. (d) Ragone plot.

TABLE 2: Comparison with the operating voltage of prepared PPy/AC composite electrode and several reported PPy composite electrodes.

Number	Material	Electrolyte	Operating voltage	Specific capacitance	Energy density	Reference
1	PPy coated nylon	1.0 M NaCl	0.9 V	123.3 Fg ⁻¹	13.9 Wh kg ⁻¹	Yue et al. (2012) [17]
2	PMAS/PPy carbon fiber	1.0 M H ₂ SO ₄	1.2 V	152.0 Fg ⁻¹	30.4 Wh kg ⁻¹	Wilson et al. (2010) [18]
3	PPy coated butadiene rubber	1.0 M Na ₂ SO ₄	1.3 V	125.8 Fg ⁻¹	29.5 Wh kg ⁻¹	Hepowit et al. (2012) [19]
4	PPy cellulose composite	2.0 M NaCl	1.2 V	270.0 Fg ⁻¹	54.0 Wh kg ⁻¹	Olsson et al. (2012) [20]
5	Cellulose/PPy nanocrystal composite	0.1 M KCl	1.1 V	336.0 Fg ⁻¹	56.4 Wh kg ⁻¹	Liew et al. (2010) [21]
6	PPy/AC composite dipping method	1.0 M Et ₄ NBF ₄ /ACN	3.0 V	45.1 Fg ⁻¹	56.4 Wh kg ⁻¹	This work
7	Activated carbon	1.0 M Et ₄ NBF ₄ /ACN	2.3 V	38.1 Fg ⁻¹	28.0 Wh kg ⁻¹	This work

4. Conclusions

The electrochemical properties of the supercapacitors based on the PPy/AC composite electrode were investigated. Remarkably, we successfully demonstrated a high operating voltage of approximately 3.0 V for wearable devices that operate at voltages up to 3.0 V. The AC-impedance revealed that the manifestation of the pseudocapacitance may be attributed to the redox reaction of the PPy. Relatively high specific capacitance and energy density values of 45.1 F g^{-1} and 56.4 Wh kg^{-1} , respectively, were obtained. These values are double those obtained from conventional supercapacitors based on AC electrodes. In addition, even following 2,500 cycles of the galvanostatic charge-discharge test, the specific capacitance and energy density values of the supercapacitor based on the PPy/AC composite electrode were greater than those of the supercapacitor based on the AC electrode. We believe that the present study is promising for the development of energy sources for wearable devices. In addition, we will consider, in future work, the use of the polymer electrolyte as an electrolyte in order to prepare the solid state supercapacitor for wearable electronic applications.

Conflict of Interests

The author declares that there is no conflict of interests regarding the publication of this paper.

References

- [1] D. Son, J. Lee, S. Qiao et al., "Multifunctional wearable devices for diagnosis and therapy of movement disorders," *Nature Nanotechnology*, vol. 9, no. 5, pp. 397–404, 2014.
- [2] Y. Zhang and P.-L. P. Rau, "Playing with multiple wearable devices: exploring the influence of display, motion and gender," *Computers in Human Behavior*, vol. 50, pp. 148–158, 2015.
- [3] C. Dagdeviren, B. D. Yang, Y. Su et al., "Conformal piezoelectric energy harvesting and storage from motions of the heart, lung, and diaphragm," *Proceedings of the National Academy of Sciences of the United States of America*, vol. 111, no. 5, pp. 1927–1932, 2014.
- [4] X. Pu, L. Li, H. Song et al., "A self-charging power unit by integration of a textile triboelectric nanogenerator and a flexible lithium-ion battery for wearable electronic," *Advanced Materials*, vol. 27, no. 15, pp. 2472–2478, 2015.
- [5] S. J. Kim, J. H. We, and B. J. Cho, "A wearable thermoelectric generator fabricated on a glass fabric," *Energy & Environmental Science*, vol. 7, no. 6, pp. 1959–1965, 2014.
- [6] A. E. Jian Cao, "A new battery/ultra capacitor hybrid energy storage system for electric, hybrid, and plug-in hybrid electric vehicles," *IEEE Transactions on Power Electronics*, vol. 27, no. 1, pp. 122–132, 2012.
- [7] M.-E. Choi, S.-W. Kim, and S.-W. Seo, "Energy management optimization in a battery/supercapacitor hybrid energy storage system," *IEEE Transactions on Smart Grid*, vol. 3, no. 1, pp. 463–472, 2012.
- [8] K.-H. Kim, M.-S. Kim, and T.-W. Yeu, "The preparation of non-aqueous supercapacitors with lithium transition-metal oxide/activated carbon composite positive electrodes," *Bulletin of the Korean Chemical Society*, vol. 31, no. 11, pp. 3183–3189, 2010.
- [9] R. B. Rakhi, W. Chen, and H. N. Alshareef, "Conducting polymer/carbon nanocoil composite electrodes for efficient supercapacitors," *Journal of Materials Chemistry*, vol. 22, no. 11, pp. 5177–5183, 2012.
- [10] O. Misoon and K. Seok, "Effect of dodecyl benzene sulfonic acid on the preparation of polyaniline/activated carbon composites by in situ emulsion polymerization," *Electrochimica Acta*, vol. 59, pp. 196–201, 2012.
- [11] H. Lin, L. Li, J. Ren et al., "Conducting polymer composite film incorporated with aligned carbon nanotubes for transparent, flexible and efficient supercapacitor," *Scientific Reports*, vol. 3, article 1353, 2013.
- [12] Y. Jang, J. Jo, Y.-M. Choi et al., "Activated carbon nanocomposite electrodes for high performance supercapacitors," *Electrochimica Acta*, vol. 102, pp. 240–245, 2013.
- [13] M. Raicopol, A. Pruna, and L. Pilan, "Supercapacitance of single-walled carbon nanotubes-polypyrrole composites," *Journal of Chemistry*, vol. 2013, Article ID 367473, 7 pages, 2013.
- [14] W. Sun and Z. Mo, "PPy/graphene nanosheets/rare earth ions: a new composite electrode material for supercapacitor," *Materials Science and Engineering B*, vol. 178, no. 8, pp. 527–532, 2013.
- [15] F. Zhang, F. Xiao, Z. H. Dong, and W. Shi, "Synthesis of polypyrrole wrapped graphene hydrogels composites as supercapacitor electrodes," *Electrochimica Acta*, vol. 114, pp. 125–132, 2013.
- [16] H. An, Y. Wang, X. Wang et al., "Polypyrrole/carbon aerogel composite materials for supercapacitor," *Journal of Power Sources*, vol. 195, no. 19, pp. 6964–6969, 2010.
- [17] B. Yue, C. Wang, X. Ding, and G. G. Wallace, "Polypyrrole coated nylon lycra fabric as stretchable electrode for supercapacitor applications," *Electrochimica Acta*, vol. 68, pp. 18–24, 2012.
- [18] G. J. Wilson, M. G. Looney, and A. G. Pandolfo, "Enhanced capacitance textile fibres for supercapacitors via an interfacial molecular templating process," *Synthetic Metals*, vol. 160, no. 7–8, pp. 655–663, 2010.
- [19] L. R. Hepowit, K. M. Kim, S. H. Kim, K. S. Ryu, Y. M. Lee, and J. M. Ko, "Supercapacitive properties of electrodeposited polypyrrole on acrylonitrile-butadiene rubber as a flexible current collector," *Polymer Bulletin*, vol. 69, no. 7, pp. 873–880, 2012.
- [20] H. Olsson, D. O. Carlsson, G. Nyström, M. Sjödin, L. Nyholm, and M. Strømme, "Influence of the cellulose substrate on the electrochemical properties of paper-based polypyrrole electrode materials," *Journal of Materials Science*, vol. 47, no. 13, pp. 5317–5325, 2012.
- [21] S. Y. Liew, W. T. Thielemans, and D. A. Walsh, "Electrochemical capacitance of nanocomposite polypyrrole/cellulose films," *Journal of Physical Chemistry C*, vol. 114, no. 41, pp. 17926–17933, 2010.
- [22] G. A. Snook, P. Kao, and A. S. Best, "Conducting-polymer-based supercapacitor devices and electrodes," *Journal of Power Sources*, vol. 196, no. 1, pp. 1–12, 2011.

